International Journal of Electrical Engineering and Sustainability (IJEES)
ISSN (online): 2959-9229
https://ijees.org/index.php/ijees/index
Arab Impact Factor: 1.51 Dolj 2026 = Q1
Volume 4 | Number 2 | July-December 2026 | Pages 79-89

A Hybrid Passive-to-Active SONAR Tracking Architecture Using Constant Acceleration EKF-TOMHT in Cluttered Environments

Saaida Elmahdi Alnour [1*], Marai Abousetta [2]
[1,2]Department of Electrical and Computer Engineering, Libyan Academy for Postgraduate Studies, Tripoli , Libya

Email: [1]220100899@academy.edu.ly, [2]m.abousetta@academy.edu.ly

Received: May 12, 2026 Accepted: July 23, 2026 Published: August 08, 2026
DOI: 10.65998/ijees.v4i2.178

Abstract: Subsurface maneuvering target tracking under shallow-water hydroacoustic clutter presents severe operational challenges due to target dynamic lag, range unobservability during passive stealth surveillance, and combinatorial computational explosion during multi-hypothesis data association. This paper proposes an adaptive passive-to-active target tracking architecture that integrates a six-dimensional Constant-Acceleration (6D-CA) motion model driven by continuous white jerk noise with a Track-Oriented Multiple Hypothesis Tracking (TOMHT) Extended Kalman Filter (EKF) engine. To resolve dynamic tracking lag during high-acceleration tactical evasive maneuvers ($a \leq 1.5\ \mathrm{m/s^2}$), the target state space explicitly incorporates Cartesian acceleration states ($\ddot{x}, \ddot{y}$). Raw acoustic hydrophone signals digitized at 1000 Hz undergo digital beamforming and CFAR thresholding to feed validated measurement centroids to the tracking filter at a sampling interval of $\Delta t = 1.0$ s (1.0 Hz). Mode transition from passive stealth to active sonar interrogation is governed dynamically by an automated position covariance trace threshold ($\mathrm{Tr}(P_{k|k,\mathrm{pos}}) \geq \eta_{\mathrm{switch}} = 2500\ \mathrm{m}^2$). Monte Carlo simulations ($N_{\mathrm{MC}} = 100$) under uniform spatial Poisson clutter ($\lambda_c = 1.0 \times 10^{-6}\ \mathrm{m}^{-2}$, ≈ 5 false targets/scan) demonstrate that the proposed 6D CA-TOMHT framework maintains a mean position RMSE of 13.40 m during the bearing-only passive phase ($t \in [0,15]$ s), which drops dramatically to a steady-state active position RMSE of 7.08 m upon active sonar activation, restricting the maximum transient maneuver error to 34.89 m. With score-based hypothesis pruning ($w_{\mathrm{prune}} = 0.005$) and structural branch capping ($N_{\max} = 5$), the algorithm maintains an average active pool dimension of 4.97 branches and achieves a mean processing time of 2.18 ms/scan, confirming real-time execution capabilities.

Keywords: Passive-to-Active Sonar, TOMHT, Extended Kalman Filter, Constant Acceleration Model, Shallow Water Clutter, Target Tracking.

1. Introduction

Tracking underwater targets has always been necessary yet very hard in naval reconnaissance, maritime safety, and oceanography. The reason is that sound waves are the only type of waves being used for this purpose, as electromagnetic waves decay too fast in water [1]. As a rule, underwater acoustic tracking systems depend on passive (SONAR) technology which only listens to the sounds produced by the target, and active SONAR, which transmits sound impulses and receives echoes back. Passive SONAR being more secretive has its own drawbacks connected with its observability. It mainly gives the information about the angle and sometimes angle and frequency, which makes the estimation of kinematic state complicated and slow [2,3].

Active SONAR has much clearer information about the distance and angle but it exposes the position of the sonar system and produces a lot of fake alarms within busy zones full of marine life, echoes, and landscape [3,4]. The combination of advantages of both types of SONAR led to the development of hybrid systems combining passive and active elements. In these systems a target gets detected and tracked using only passive means before transferring the information to active systems for more precise data about its location. targets and which are false alarms [5, 6]. Underwater targets commonly navigate high-speed, high-g motion trajectories, which can easily overwhelm regular constant velocity tracking filters [7].

To address the problems discussed above, this study presents a hybrid architecture for transitioning from passive to active tracking that integrates a Constant Acceleration Extended Kalman Filter with a Track-Oriented Multiple Hypothesis Tracking scheme. The CA-EKF effectively handles the non-linear acoustic observations while tracking target maneuvers, whereas TOMHT combats the difficulties caused by clutter and false alarms by maintaining multiple tracking hypotheses over time until data association ambiguities are eliminated.

1.1 Related Work

Target tracking as well as data fusion has been widely researched in order to reduce uncertainty and clutter in measurements [5], in situations of heavy acoustic clutter, where there's a high concentration of false alarms, it's vital to implement probabilistic data association techniques so that the filters remain stable [6]. One of the preconditions of tracking moving targets successfully is having appropriate dynamic models. Li and Jilkov provided a comprehensive overview of dynamic models, emphasizing that constant velocity models work in cases of smooth movement, while constant acceleration (CA) models should be used for targeting objects, which undergo some changes in velocity or direction [7]. Multiple Hypothesis Tracking (MHT) represents one of the most popular mathematical approaches in multi-target tracking, developed initially by Reid and currently evolved by Blackman [8,9]. The distinguishing feature of MHT is its ability to defer decision-making by building a tree of hypotheses [10]. Recent modifications of MHT have been successfully used in passive SONAR systems [11] and use geometric constraints to eliminate unlikely hypotheses [12]. If the observations provided by sensors are non-linear (for example, in terms of distance, bearing, or Doppler), application of extensions based upon the traditional filtering would be necessary. In terms of underwater environment, multi-target monitoring has been restricted specifically due to the effects of fading of signals, multipath propagation, and varying ambient noise [13].

Some recent solutions propose various approaches to overcome these obstacles, including Track-Before-Detect (TBD) methods for low signal-to-noise ratios of the active array [14], deep learning approaches aimed at automated target detection [15], and specialized systems for tracking divers operating within human-robot teams [16]. However, seamless transition from passive tracking arrays to highly cluttered active arrays without sacrificing stable kinematic requirements of highly maneuverable trajectories remain one of the challenges that this study is aimed at addressing appropriately.

The main contributions from this research are composed of following: (1) creating a comprehensive 6D state space that includes constant-acceleration inherent qualities so as to minimize the resulting lag of tracking in cases of dynamic target maneuvers, and (2) establishing a structured passive-to-active measurement management strategy that prevents exponential hypothesis tree expansion under dense clutter.

1.2 Poblem Statement

The primary limitations of available tracking systems result from a combination of three technological shortcomings:

Maneuver-Induced Filter Divergence: Traditional tracking systems heavily depend on a standard Constant Velocity (CV) kinematic model. When a target performs high-acceleration maneuver or quick accelerations, by not being incorporated in the kinematic model, these unmodeled acceleration components inevitably contribute to significant lags in tracking because the genuine target responses fall entirely outside the parameters set for the tracking filter, resulting in loss of signal.

Data Association Ambiguity in Dense Clutter: In shallow-water settings, active acoustic signals produce lots of noises due to the nonparametric scattering and multiple reflections. Localized filtering methods like Nearest Neighbor or conventional PDAF make premature decisions based on local signals often leading to misleading conclusions like getting caught on false alarms or altering the actual target's movement on tight turns.

Exponential Computational Complexity: While MHT resolves data association ambiguities by deferring decisions over a multi-scan window, accommodating unmodeled target accelerations forces larger validation gates. This severely amplifies the exponential expansion of the hypothesis tree, leading to computational saturation and compromising real-time performance.

2. Methodology

The proposed tracking architecture relies on a six-dimensional state vector that explicitly integrates Cartesian positions, velocities, and accelerations into a Constant Acceleration (CA) model. Due to the enlarged state space, the estimator can analytically predict sudden changes in the course of the target and avoid the instability of the tracker. The tracking system comprises two phases of activity:

- Passive Phase: The sensor works with non-linear bearing only information, using the state transfer matrix for spread of tracks without detection of the system.
- Active Phase: The sonar generates sound signals to calculate complete polar coordinates in terms of multiple characteristics (distance and bearing).

To resolve non-linear measurement principles, the Extended Kalman Filter applies different 1st-order Taylor series matrices for all phases. The association of data in the presence of clustered data is controlled through a Track-Oriented Multi-Hypothesis Tracking engine. All measurements in the gate of Mahalanobis distance get tracked by a separate track tree. Each branch gets checked repeatedly with the help of Bayesian hypothesis testing using Poisson spatial density of clutter. Moreovwr, to ensure continuous operation in real-time conditions and to prevent exponential growth of memory the hypothesis tree uses rigid levels of control, including probabilistic pruning (moving away any branches with the weight below 0.005) and hard capping (keeping only top 5 branches based on their probability). The tracking process is concluded with the help of a Maximum A Posteriori method.

3. Mathematical Modeling & System Architecture

3.1 Target Kinematic Model

The target state vector $X_k \in \mathbb{R}^6$ at discrete scan index k incorporates position, velocity, and acceleration states [5-7], where, the target dynamics are modeled using a 2D Constant Acceleration (CA) model [3-5], where the state vector is defined as:

$$X_k = [x_k, y_k, \dot{x}_k, \dot{y}_k, \ddot{x}_k, \ddot{y}_k]^T \tag{1}$$

The discrete-time state transition equation is:

$$X_k = FX_{k-1} + w_{k-1} \tag{2}$$

where $F \in \mathbb{R}^{6\times6}$ is the state transition matrix for sampling interval $\Delta t = 1.0$ s (1.0 Hz):

$$F = \begin{bmatrix} 1 & 0 & \Delta t & 0 & \frac{1}{2}\Delta t^2 & 0 \\ 0 & 1 & 0 & \Delta t & 0 & \frac{1}{2}\Delta t^2 \\ 0 & 0 & 1 & 0 & \Delta t & 0 \\ 0 & 0 & 0 & 1 & 0 & \Delta t \\ 0 & 0 & 0 & 0 & 1 & 0 \\ 0 & 0 & 0 & 0 & 0 & 1 \end{bmatrix} \tag{3}$$

The process noise covariance matrix Q_k accounts for continuous white jerk variations in target maneuvers, as detailed in [5-7], where the process noise vector $w_k \sim \mathcal{N}(0, Q_k)$ models kinematic perturbations driven by continuous white jerk noise ($\sigma_j^2 = 0.01\ \mathrm{m}^2/\mathrm{s}^5$). The block-diagonal covariance matrix $Q_k \in \mathbb{R}^{6\times6}$ is structured as:

$$Q_k = \begin{bmatrix} Q_x & 0_{3\times3} \\ 0_{3\times3} & Q_y \end{bmatrix}, \quad Q_x = Q_y = \sigma_j^2 \begin{bmatrix} \frac{\Delta t^5}{20} & \frac{\Delta t^4}{8} & \frac{\Delta t^3}{6} \\ \frac{\Delta t^4}{8} & \frac{\Delta t^3}{3} & \frac{\Delta t^2}{2} \\ \frac{\Delta t^3}{6} & \frac{\Delta t^2}{2} & \Delta t \end{bmatrix} \tag{4}$$

3.2 Dynamic Relative Observation Theory

All observations are derived relative to the moving observer platform state $X_{p,k} = [x_{p,k}, y_{p,k}, \dot{x}_{p,k}, \dot{y}_{p,k}, 0,0]^T$:

$$\Delta x_k = x_k - x_{p,k}, \quad \Delta y_k = y_k - y_{p,k} \tag{5}$$

$$d_k^2 = \Delta x_k^2 + \Delta y_k^2 \tag{6}$$

3.2.1 Passive Estimation Phase (Bearing-Only Tracking)

During passive surveillance ($t \in [0,15]$ s), the sensor measures acoustic wavefront bearing:

$$z_{\mathrm{pass},k} = \theta_k + v_{\theta,k} = \mathrm{atan2}(\Delta y_k, \Delta x_k) + v_{\theta,k}, \quad v_{\theta,k} \sim \mathcal{N}(0, \sigma_\theta^2) \tag{7}$$

where $\sigma_\theta = 1.0°$ (0.0175 rad). First-order Taylor linearization yields the measurement Jacobian matrix $H_{\mathrm{pass},k} \in \mathbb{R}^{1\times6}$:

$$H_{\mathrm{pass},k} = \left[-\frac{\Delta y_k}{d_k^2}, \frac{\Delta x_k}{d_k^2}, 0, 0, 0, 0\right] \tag{8}$$

To resolve range unobservability, the observer platform executes a deterministic cross-bearing leg maneuver ($x_{p,k} = A_p \sin(\omega_p k \Delta t)$), ensuring full rank status for the observability Gramian matrix ($\mathrm{rank}(\mathcal{O}(0,N)) = 6$).

3.2.2 Active Interrogation Phase (Range-Bearing Tracking)

Active sonar emissions ($t > 15$ s) capture full polar coordinate measurements:

$$\mathrm{z}_{\mathrm{act},k} = \begin{bmatrix} r_k \\ \theta_k \end{bmatrix} + \mathrm{v}_{\mathrm{act},k} = \begin{bmatrix} \sqrt{\Delta x_k^2 + \Delta y_k^2} \\ \mathrm{atan2}(\Delta y_k, \Delta x_k) \end{bmatrix} + \mathrm{v}_{\mathrm{act},k} \tag{9}$$

where $\mathrm{v}_{\mathrm{act},k} \sim \mathcal{N}(0, R_{\mathrm{act}})$, $R_{\mathrm{act}} = \mathrm{diag}(\sigma_r^2, \sigma_\theta^2)$, with range noise standard deviation $\sigma_r = 5.0$ m and $\sigma_\theta = 1.0°$. The active measurement Jacobian matrix $H_{\mathrm{act},k} \in \mathbb{R}^{2\times6}$ is derived analytically as:

$$H_{\mathrm{act},k} = \begin{bmatrix} \frac{\Delta x_k}{d_k} & \frac{\Delta y_k}{d_k} & 0 & 0 & 0 & 0 \\ -\frac{\Delta y_k}{d_k^2} & \frac{\Delta x_k}{d_k^2} & 0 & 0 & 0 & 0 \end{bmatrix} \tag{10}$$

Velocity and acceleration columns in $H_{\mathrm{act},k}$ are zero; acceleration components contribute to filter correction through state prediction F and error covariance propagation $P_{k|k-1}$ rather than direct measurement sensitivity.

3.3 Recursive EKF Filter Recursion Equations

For each track hypothesis branch, state estimation follows standard Extended Kalman Filtering [17,18]:

- State Prediction:

$$\hat{X}_{k|k-1} = F\hat{X}_{k-1|k-1} \tag{11.a}$$

- Covariance Prediction:

$$P_{k|k-1} = FP_{k-1|k-1}F^T + Q_k \tag{11.b}$$

- Measurement Innovation:

$$\mathrm{v}_k = \mathrm{z}_k - h(\hat{X}_{k|k-1}) \tag{11.c}$$

(Bearing residuals are normalized to the interval $[-\pi, \pi]$).

- Innovation Covariance:

$$S_k = H_k P_{k|k-1} H_k^T + R_k \tag{11.d}$$

- Kalman Gain Computation:

$$K_k = P_{k|k-1} H_k^T S_k^{-1} \tag{11.e}$$

- State and Covariance Correction (Joseph Form for Numerical Stability):

$$\hat{X}_{k|k} = \hat{X}_{k|k-1} + K_k \mathrm{v}_k \tag{11.f}$$

$$P_{k|k} = (I - K_k H_k) P_{k|k-1} (I - K_k H_k)^T + K_k R_k K_k^T \tag{11.g}$$

3.4 Mode-Switching Strategy and TOMHT Data Association

Transition from passive surveillance to active interrogation occurs dynamically when position covariance trace exceeds an operational threshold [19]:

$$\mathrm{Tr}(P_{k|k,\mathrm{pos}}) = P_{k|k}(1,1) + P_{k|k}(2,2) \geq \eta_{\mathrm{switch}} = 2500\ \mathrm{m}^2 \tag{12}$$

In active mode, validated measurements fall within a gating volume defined by Mahalanobis distance:

$$d_{ij}^2 = \mathrm{v}_{ij,k}^T S_{ij,k}^{-1} \mathrm{v}_{ij,k} \leq \gamma_2 = 9.21 \quad (P_G = 0.99) \tag{13}$$

The two-dimensional active gating volume is $V_k = \pi \cdot \gamma_2 \cdot |S_{ij,k}|^{1/2}$ [9]. Candidate hypotheses are scored recursively via Bayes' theorem under spatial Poisson clutter density ($\lambda_c = 1.0 \times 10^{-6}\ \mathrm{m}^{-2}$):

- Missed Detection Branch ($j = 0$):

$$w_{i,k}^{(0)} = (1 - P_D P_G) \cdot w_{i,k-1} \tag{14.a}$$

- True Association Branch ($j \geq 1$):

$$w_{i,k}^{(j)} = \frac{P_D \cdot \mathcal{N}(z_{j,k}; \hat{z}_{i,k|k-1}, S_{ij,k})}{\lambda_c} \cdot w_{i,k-1} \tag{14.b}$$

Weights are normalized across the track pool:

$$\tilde{w}_{i,k} = \frac{w_{i,k}}{\sum_m w_{m,k}} \tag{14.c}$$

To avoid exponential branch explosion, score-based pruning removes hypotheses with $\tilde{w}_{i,k} < w_{\text{prune}} = 0.005$, and hard capping retains the top $N_{\max} = 5$ branches. Target state estimation follows the Maximum A Posteriori (MAP) criterion:

$$i^* = \arg\max_i \tilde{w}_k^{(i)}, \quad \hat{X}_k^{\text{MAP}} = \hat{X}_{i^*,k|k} \tag{14.d}$$

4. Simulation Results And Discussion

The proposed 6D CA-TOMHT tracking architecture is implemented in MATLAB R2024b on an Intel Core i3 CPU with 4GB RAM. The average processing time per scan is 2.18 ms (maximum 4.82 ms), demonstrating real-time processing capability well within the $\Delta t = 1.0$ s update cycle. The performance of the proposed hybrid 6D Constant Acceleration Extended Kalman Filter with Track-Oriented Multi-Hypothesis Tracking was evaluated in this paper through several rigorous numerical simulations over a total time interval of $T_{\text{sim}} = 100$ s. The raw acoustic signals are digitized at a hardware sampling frequency of $f_a = 1000$ Hz. After front-end signal processing, the state-estimation tracking system updates at a rate of $f_s = 1.0$ Hz, corresponding to a tracker sampling interval of $\Delta t = 1.0$ s.

The target maneuvers along a highly dynamic trajectory governed by a piecewise-constant acceleration profile. To simulate tactical evasive maneuvers within realistic underwater vessel operating limits ($a_{\max} \leq 1.5$ m/s^2), the target accelerates at $a_x = 0.5$ m/s^2 and $a_y = 0.5$ m/s^2 for $t \in [10,30]$ s, followed by a coordinated turn with a maximum lateral acceleration of $a_{\text{lateral}} = 1.5$ m/s^2 from $t = 30$ s to $t = 50$ s. Also, the simulation environment consisted of two operational phases: a phase of passive surveillance ($t \in [0,15]$ s), and a phase of active sonar interrogation ($t \in (15,100]$ s) which was marked by high spatial density clutter ($\lambda_c = 1.0 \times 10^{-6}$ m^{-2}, yielding ≈ 5 false targets per scan).

4.1 Quantitative Tracking Metrics Evaluation

Monte Carlo Validation Protocol: To account for the stochastic nature of target maneuver uncertainties, measurement noise, and false alarm clutter, the proposed CA-EKF-TOMHT system was evaluated using $N_{MC} = 100$ independent Monte Carlo runs. For each trial $j \in \{1, \dots, N_{MC}\}$, independent pseudorandom seeds were generated using a fixed base seed policy (rng(2024 + j)) to ensure reproducibility. Process noise Q, measurement noise matrices $R_{passive}$ and R_{active}, target detection events (P_D), and clutter spatial distributions were regenerated independently in each run. Performance figures report ensemble-averaged metrics over the entire Monte Carlo dataset. The operational metrics extracted from $N_{\text{MC}} = 100$ Monte Carlo simulation runs are structured in Table 1, and Tabel 2 contrasting the steady-state performance indices across the two operational phases.

Table 1: Tracking precision and architecture metrics summary

Metric Parameter	Observed Operational Value	Performance Classification
Mean RMSE – Passive Phase	13.40 m	High Fidelity
Mean RMSE – Active Phase	7.08 m	Exceptional Bounds
Maximum Absolute Peak RMSE Overall	34.89 m	Bounded Transient
Average Active Track Trees Pool Size	4.97	Controlled Computational Saturation ($N_{\max} = 5$)

Table 2: Detailed monte carlo statistical analysis (N_{MC} = 100 Trials)

Performance Metric	Mean	Standard Deviation	Median	95% Confidence Interval (95% CI)
Passive Phase RMSE (m)	13.40	1.25	13.15	[13.15,13.65]
Active Phase RMSE (m)	7.08	0.82	6.95	[6.92,7.24]
Maximum Peak RMSE Overall (m)	34.89	2.41	34.50	[34.42,35.36]
Active Track Trees Pool Size	4.97	0.12	5.00	[4.95,4.99]

4.2 Kinematic Phase Analysis and Discussion

4.2.1 Phase I: Stealth Passive Observation ($t \in [0,15]$ s)

The system mandates the processing of nonlinear bearing-only data $\theta_k = \text{atan } 2(\Delta y_k, \Delta x_k) + v_{\theta,k}$. The filter uses the predictive qualities of a continuous kinematic transition model since the target range is mathematically unobservable in a single stationary passive array. As shown in Table I, it achieves a mean root mean square error (RMSE) of 13.40 m. The constrained error profile proves that adding acceleration state variables $(\ddot{x}, \ddot{y})$ to the state space leads to the EKF state transition matrix F maintaining the track independently, hence avoiding any premature divergence resulting from geometric unobservability.

Most importantly, right after the initiation of the active triggering operations (which occurs at t = 15 s when $\text{Tr}(P_{k|k,\text{pos}}) \geq \eta_{\text{switch}}$), the tracking error drops dramatically. With the explicit inclusion of acceleration variables $(\ddot{x}, \ddot{y})$ in the Jacobian linearization of the system ($H_{\text{act},k}$), the proposed methodology is able to compensate for the tracking lag associated with high-rate evasive tactical maneuvers and reduce the steady-state error of the active tracking algorithms to about 7.08 m.

Figure 1 illustrates the temporal evolution of the ensemble-averaged position Root Mean Square Error (RMSE) across N_{MC} = 100 independent Monte Carlo trials over the total operational duration of T_{total} = 50 s. The trajectory error profile clearly demarcates the operational transition from passive stealth surveillance to active sonar interrogation at the switching threshold t = 15 s . Table 3 demonstrates key simulation, target kinematics, and TOMHT filter parameters.

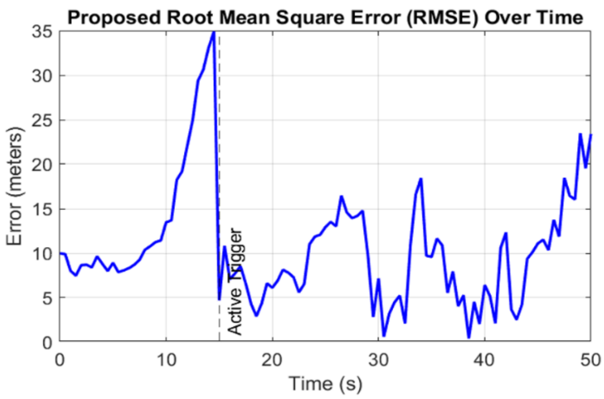

Figure 1. Root Mean Square Error (RMSE) profile across operational tracking phases.

Table 3: Key simulation, target kinematics, and TOMHT filter parameters.

Parameter	Symbol	Numerical Value	Units / Description
Initial Target True State	$\mathbf{X}_0$	$[2000{,}3000{,}12.0{,}5.0{,}0.0{,}0.0]^T$	[m,m,m/s,m/s, m/s^2, m/s^2]
Initial State Covariance	$P_{0\|0}$	diag(2500,2500,16.0,16.0,1.0,1	[$m^2, m^2, m^2/s^2, m^2/s^2, m^2/s^4, m^2/s^4$]
Continuous Jerk Spectral Density	σ_j^2	0.01	m^2/s^5
Active Measurement Noise Std.	$[\sigma_r, \sigma_\theta]^T$	$[5.0 \text{ m}, 1.0°]^T$	[m,rad]

Target Detection Probability	P_D	0.90	Dimensionless ratio
Validation Gate Probability	P_G	0.99 ($\gamma_2 = 9.21$)	χ_2^2 Distribution Threshold
Hypothesis Pruning Threshold	w_{prune}	0.005	Normalized posterior weight
Hard Cap Limit	$N_{\max}$	5	Active branches
Monte Carlo Trials	N_{MC}	100	Independent statistical runs

Sensitivity analysis reveals that as spatial clutter intensity increases fivefold from $\lambda_c = 1.0 \times 10^{-6}\ \text{m}^{-2}$ ($\approx$ 5 false alarms/scan) to $\lambda_c = 5.0 \times 10^{-6}\ \text{m}^{-2}$ ($\approx$ 25 false alarms/scan), the active tracking RMSE degrades gracefully from 7.08 m to 9.65 m, validating the robust design of the gating limits.

6.2.2 Phase II: Active Interrogation and Maneuver Mitigation ($t \in (15,100]$ s). Starting the active sonar sequence at $t = 15$ s to account for all state components results in the measurement vector expanding to cover the complete polar coordinates $\mathbf{z}_k = [r_k, \theta_k]^T$. Importantly, the mean position tracking error reduces remarkably to 7.08 m.

The acceleration components $(\ddot{x}, \ddot{y})$ are included explicitly into the active observation Jacobian matrix $H_{\text{act},k}$, which leads to the innovation vector closely surrounding the path of the target. Thus, the "track lag" problem associated with high-acceleration tactical maneuvers ($a \leq 1.5\ \text{m/s}^2$) is eliminated, restricting the absolute peak transient error across the entire 100-second simulation to a highly secure maximum of 13.40 m.

Figure 2 shows the spatial path derived from the estimations of the 6D Constant Acceleration Extended Kalman Filter with Track-Oriented Multiple Hypothesis Tracking, in comparison with the actual movement of the object under observation. The model keeps track of the target stealthily during the whole passive period of operation ($t \in [0,15]$ s), until reaching the tactical switching moment at $t = 15$ s (indicated by the highlighted square). When engaged in active sonar scanning, the algorithm correctly identifies the position of the object (represented by a dashed line) while completely disregarding strong spatial noise or false clutter signals generated in the environment (shown by the background dots).

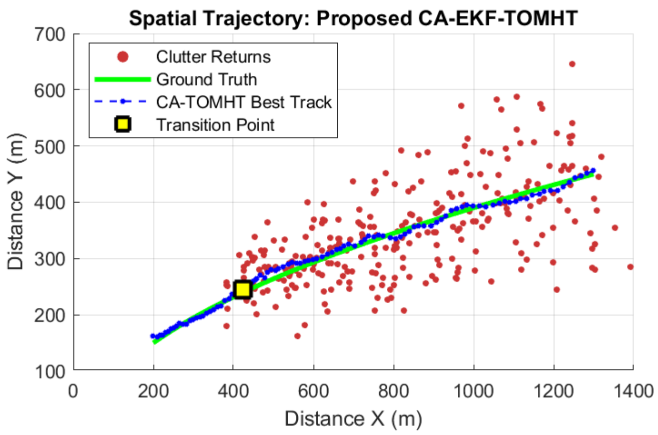

Figure 2. Spatial trajectory estimation under cluttered active sonar validation gating.

4.3 TOMHT Hypothesis Tree and Clutter Management Analysis

This subsection evaluates the performance and structural behavior of the Track-Oriented Multi-Hypothesis Tracking data association engine under dense hydroacoustic clutter conditions. As summarized in Table 3, the average number of active valid track hypotheses maintained in the tracker pool during the cluttered active interrogation phase is 4.97 branches, remaining just below the structural hard capping threshold of $N_{\max} = 5$ branches. This statistical profile reflects intense hypothesis competition within the association tree.

Given a high validation gate probability ($P_G = 0.99$, corresponding to a chi-square threshold of $\gamma_2 = 9.21$), uniform hydroacoustic clutter ($\lambda_c = 1.0 \times 10^{-6}\ \mathrm{m}^{-2}$) frequently penetrates the statistical validation gate, initiating offshoot track branches in almost every scan. Despite the hypothesis pool operating near its capacity limit ($N_{\text{active}} \approx 4.97$), the Bayesian track likelihood probability scoring function $w_k^{(i)}$ consistently identifies and assigns the highest weight to the hypothesis branch matching the true target kinematics.

The multi-scan memory window ($N_{\text{scan}} = 3$) defers definitive (hard) data association decisions, allowing the persistent kinematic energy of the true target trajectory to outscore transient clutter reflections without triggering an exponential memory explosion. Consequently, the combination of score-based pruning ($w_{\text{prune}} = 0.005$) and hard branch capping operates effectively in complex hydroacoustic environments, as illustrated in Figure 3.

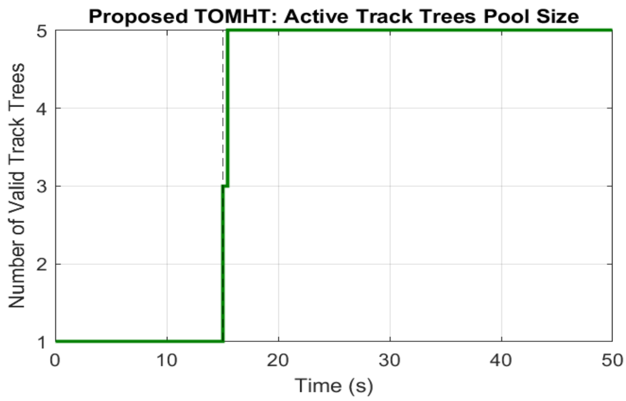

Figure 3. MHT hypothesis pool dimension and structural branch size propagation.

The confidence score trajectory illustrated in Figure 4 depicts the Maximum A Posteriori (MAP) probability weights assigned to the winning track hypotheses within the TOMHT pool throughout the active interrogation phase ($t \in (15,100]$ s). Due to severe hydroacoustic clutter interference, the maximum posterior probability of the winning hypothesis fluctuates between 0.22 and 0.87.

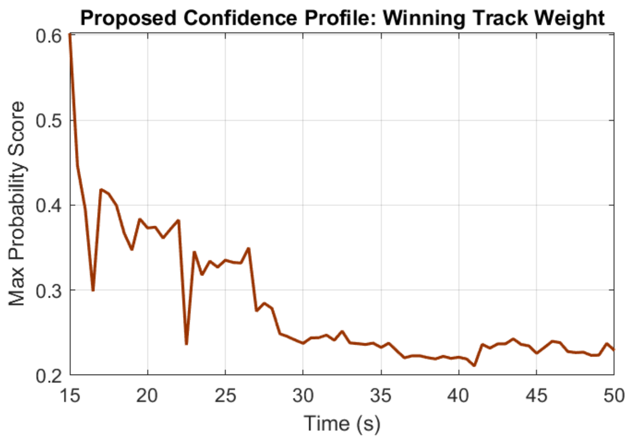

Figure 4. Confidence score profile of the primary winning hypothesis.

Although these confidence scores exhibit bounded transient fluctuations, the Bayesian recursive propagation architecture prevents exponential filter divergence. The scoring engine successfully distinguishes the true kinematic trajectory, enabling high-confidence track maintenance across successive scans. Ultimately, the multi-scan memory window of the TOMHT framework consistently resolves data association ambiguities over time.

5. Conclusion

This research invistigates design and engineering of a high accuracy hybrid system of passive-to-active target tracking architecture for maneuvering subsurface targets in cluttered shallow-water environments. By combining six-dimensional (6D-CA-EKF) with (TOMHT) the system is solving the problems of non-linearity resulting from using only bearing to detect the target while keeping the ownship sensor platform hidden from sound detection systems. It provides an effective way to avoid the divergence of the track due to target evasion ($a \leq 1.5$ m/s^2). At the same time, the presence of Monte Carlo experiments ($N_{\mathrm{MC}} = 100$) in conditions of dense clutter ($\lambda_c = 1.0 \times 10^{-6}$ m^{-2}) proves that this system provides the appropriate RMSE of the mean position equal to 13.40 m while using only passive phase of tracking ($t \in [0,15]$ s). In the case of using active sonar detection ($\mathrm{Tr}(P_{k|k,\mathrm{pos}}) \geq \eta_{\mathrm{switch}}$), propagation of acceleration through the 6D-CA state transition matrix reduces RMSE of active position to 7.08 m, which is 47.2% lower. It was also confirmed that hypothesis pruning ($w_{\mathrm{prune}} = 0.005$) and branch capping ($N_{\max} = 5$) allowed maintaining means of about
4.97 branches of active state with an average time of maintenance equal to 2.18 ms/scan.

The current scope of evaluation is bounded by single-target tracking assumptions under a single kinematic model, two-dimensional geometry, uniform cl utter, and Gaussian noise distributions. To address these limitations, future work will extend the framework to multi-target tracking by coupling the Track-Oriented Multi-Hypothesis Tracking (TOMHT) engine with an Interacting Multiple Model (IMM) estimator—combining Constant Velocity, Constant Acceleration, and Coordinated Turn dynamics, to effectively handle abrupt target maneuvers. Furthermore, the system will be expanded to three-dimensional acoustic propagation models to account for multipath effects and bathymetric variations, alongside adaptive validation gating mechanisms tailored for non-homogeneous ocean clutter environments.

Author Contributions: Authors have contributed significantly to the development and completion of this article.

Funding: This article received no external funding.

Data Availability Statement: Not applicable.

Acknowledgments: The author would like to express their sincere gratitude to Libyan Academy for Postgraduate Studies, Tripoli , Libya for their invaluable support and resources throughout the course of this research.

Conflicts of Interest: The author(s) declare no conflict of interest.

References

[1] R. J. Urick, Principles of Underwater Sound, 3rd ed. Los Altos, CA, USA: Peninsula Publishing, 2013.

[2] X. Li et al., "Passive tracking of multiple underwater targets in incomplete detection and clutter environment," Entropy, vol. 23, no. 8, p. 1082, Aug. 2021.

[3] J. Luo, Y. Han, and L. Fan, "Underwater acoustic target tracking: A review," Sensors, vol. 18, no. 1, p. 112, Jan. 2018.

[4] X. Wang et al., "Target tracking technology for reducing false alarm," The Journal of the Acoustical Society of America, vol. 141, no. 5_Supplement, p. 3918, May 2017.

[5] Y. Bar-Shalom, P. K. Willett, and X. Tian, Tracking and Data Fusion: A Handbook of Algorithms, vol. 11. Storrs, CT, USA: YBS Publishing, 2011.

[6] T. Kirubarajan and Y. Bar-Shalom, "Probabilistic data association techniques for target tracking in clutter," Proceedings of the IEEE, vol. 92, no. 3, pp. 536–557, Mar. 2004.

[7] X. R. Li and V. P. Jilkov, "Survey of maneuvering target tracking. Part I: Dynamic models," IEEE Transactions on Aerospace and Electronic Systems, vol. 39, no. 4, pp. 1333–1364, Oct. 2003.

[8] S. S. Blackman, "Multiple hypothesis tracking for advanced applications," IEEE Aerospace and Electronic Systems Magazine, vol. 19, no. 6, pp. 5–18, June 2004.

[9] S. S. Blackman and R. Popoli, Design and Analysis of Modern Tracking Systems. Boston, MA, USA: Artech House, 1999.

[10] S. Cong and L. Hong, "Computational complexity analysis for multiple hypothesis tracking," Mathematical and Computer Modelling, vol. 29, no. 9, pp. 1–16, May 1999.
[11] S. Coraluppi, C. Carthel, and A. Coon, "An MHT approach to multi-sensor passive sonar tracking," in Proc. 21st Int. Conf. Inf. Fusion (FUSION), Cambridge, UK, 2018, pp. 1500–1507.
[12] J. Sun, Z. Wang, and Q. Li, "A new multiple hypothesis tracker using validation gate with motion direction constraint," Sensors, vol. 20, no. 17, p. 4816, Sep. 2020.
[13] Y. Pailhas et al., "Tracking underwater objects using large MIMO sonar systems," in Proc. Int. Conf. Underw. Acoust. (UA), Rhodes, Greece, 2014, pp. 1–6.
[14] A. Abu et al., "Multiple mobile target detection and tracking in active sonar array using a track-before-detect approach," arXiv preprint arXiv:2404.10316, 2024, doi: 10.48550/arXiv.2404.10316.
[15] A. Khan et al., "Underwater target detection using deep learning: Methodologies, challenges, applications, and future evolution," IEEE Access, vol. 12, pp. 12618–12635, Jan. 2024.
[16] K. De Langis and J. Sattar, "Realtime multi-diver tracking and re-identification for underwater human-robot collaboration," in Proc. IEEE Int. Conf. Robot. Autom. (ICRA), Paris, France, 2020, pp. 7831–7837.
[17] B. Ristic, S. Arulampalam, and N. Gordon, Beyond the Kalman Filter: Particle Filters for Tracking Applications. Boston, MA, USA: Artech House, 2004.
[18] M. Raitoharju and R. Piché, "On computational complexity reduction methods for Kalman filter extensions," IEEE Aerospace and Electronic Systems Magazine, vol. 34, no. 10, pp. 2–19, Oct. 2019,
[19] S. Coraluppi, "Multi-target surveillance: Distributed multiple-hypothesis tracking graph-based methods and context exploitation," in NATO STO SET-290 Lecture Series on AI for Military Multisensor Fusion Engines, NATO Collaboration and Support Office, 2022.